

Blue or Green Glowing Crystals of the Cation $[\text{Au}\{\text{C}(\text{NHMe})_2\}_2]^+$. Structural Effects of Anions, Hydrogen Bonding, and Solvate Molecules on the Luminescence of a Two-Coordinate Gold(I) Carbene Complex

Daniel Rios, David M. Pham, James C. Fettinger, Marilyn M. Olmstead, and Alan L. Balch*

Department of Chemistry, University of California, Davis, California 95616

Received December 21, 2007

Depending upon the crystallization conditions, $[\text{Au}\{\text{C}(\text{NHMe})_2\}_2](\text{AsF}_6)$ forms colorless crystals that display a blue or green luminescence. The difference involves the type of solvate molecule that is incorporated into the crystal and the structure of the chains of cations that are formed upon crystallization. The crystallographically determined structures of blue-glowing $[\text{Au}\{\text{C}(\text{NHMe})_2\}_2](\text{AsF}_6) \cdot 0.5(\text{benzene})$, blue-glowing $[\text{Au}\{\text{C}(\text{NHMe})_2\}_2](\text{AsF}_6) \cdot 0.5(\text{acetone})$, green-glowing $[\text{Au}\{\text{C}(\text{NHMe})_2\}_2](\text{AsF}_6) \cdot 0.5(\text{chlorobenzene})$, and blue-glowing, solvate-free $[\text{Au}\{\text{C}(\text{NHMe})_2\}_2](\text{EF}_6)$, $\text{E} = \text{P, As, Sb}$ are reported. All pack with the cations forming extended columns, which may be linear or bent, but all show significant aurophilic interactions. The blue-glowing crystals have ordered stacks of cations with some variation in structural arrangement whereas the green-glowing crystals have disorder in their stacking pattern. Although there is extensive hydrogen bonding between the cations and anions in all structures, in the solvated crystals, the solvate molecules occupy channels but make no hydrogen-bonded contacts. The emission spectra of these new salts taken at 298 and 77 K are reported.

Introduction

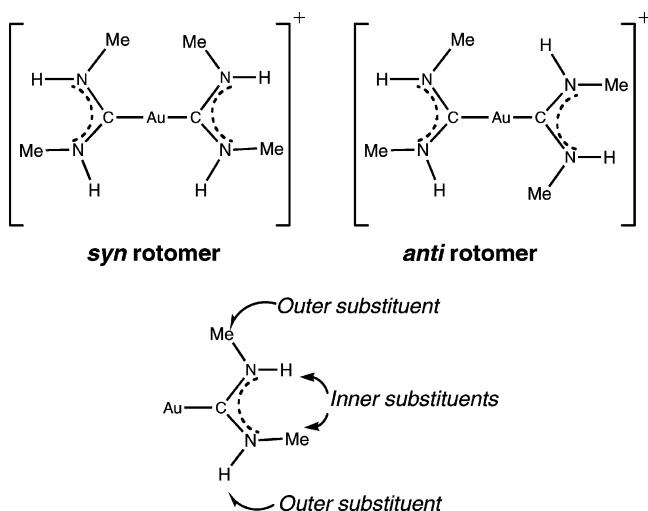
Gold(I) complexes are frequently colorless, two-coordinate compounds that can display interesting luminescence properties.¹ For such two-coordinate gold(I) complexes, a combination of correlation and relativistic effects^{2,3} produces an attractive $\text{Au}\cdots\text{Au}$ interaction with a bond strength comparable to that of a hydrogen bond.⁴ Aurophilic attractions have been implicated in the luminescence from several types of gold(I) complexes,⁵ (e.g., emission from ligand-bridged dimers,⁶ the novel tunable luminescence from $[\text{Au}(\text{CN})_2]^-$,⁷ solvoluminescence,⁸ variable emission from $[\text{Au}(\text{SCN})_2]^-$,⁹

and a potassium ion sensor¹⁰). In molecular orbital (MO) terms, the self-association of such d^{10} complexes can be ascribed to the interaction of the d_{z^2} orbitals to form a filled

* To whom correspondence should be addressed. E-mail: albalch@ucdavis.edu.

- (1) (a) Balch, A. L. *Struct. Bonding (Berlin)* **2007**, *123*, 1. (b) Forward, J. M.; Fackler, J. P., Jr.; Assefa, Z. In *Optoelectronic Properties of Inorganic Compounds*; Fackler, J. P., Jr., Roundhill, D. M., Eds. Plenum Press: New York, 1999; p 195.
- (2) (a) Schmidbaur, H. *Chem. Soc. Rev.* **1995**, *24*, 391. (b) Grohmann, A.; Schmidbaur, H. In *Comprehensive Organometallic Chemistry II*; Abel, E. W., Stone, F. G. A., Wilkinson, G., Eds.; Elsevier: Oxford, 1995; Vol. 3, pp 1.
- (3) (a) Pyykkö, P. *Angew. Chem., Int. Ed.* **2004**, *43*, 4412. (b) Pyykkö, P. *Chem. Rev.* **1997**, *97*, 597.
- (4) (a) Schmidbaur, H.; Graf, W.; Müller, G. *Angew. Chem., Int. Ed. Engl.* **1988**, *27*, 417. (b) Harwell, D. E.; Mortimer, M. D.; Knobler, C. B.; Anet, F. A. L.; Hawthorne, M. F. *J. Am. Chem. Soc.* **1996**, *118*, 2679.
- (5) Fackler, J. P., Jr. *Inorg. Chem.* **2002**, *41*, 6959.

- (6) (a) For some examples see: King, C.; Wang, J.-C.; Khan, M. N. I.; Fackler, Jr., J. P. *Inorg. Chem.* **1989**, *28*, 2145. (b) Che, C.-M.; Kwong, H.-L.; Yam, V. W.-W.; Cho, C.-K. *J. Chem. Soc., Chem. Commun.* **1989**, 885. (c) Fu, W.-F.; Chan, K.-C.; Miskowski, V. M.; Che, C.-M. *Angew. Chem., Int. Ed.* **1999**, *38*, 2783. (d) Che, C.-M.; Wong, W.-T.; Lai, T.-F.; Kwong, H.-L. *J. Chem. Soc., Chem. Commun.* **1989**, 243. (e) Leung, K. H.; Phillips, D. L.; Tse, M. C.; Che, C. M.; Miskowski, V. M. *J. Am. Chem. Soc.* **1999**, *121*, 4799.
- (7) (a) Rawashdeh-Omary, M. A.; Omary, M. A.; Patterson, H. H.; Fackler, J. P., Jr. *J. Am. Chem. Soc.* **2001**, *123*, 11237. (b) Rawashdeh-Omary, M. A.; Omary, M. A.; Patterson, H. H. *J. Am. Chem. Soc.* **2000**, *122*, 10371. (c) Fischer, P.; Mesot, J.; Lucas, B.; Ludi, A.; Patterson, H.; Hewat, A. *Inorg. Chem.* **1997**, *36*, 2791. (d) Hettiarachchi, S. R.; Rawashdeh-Omary, M. A.; Kanan, S. M.; Omary, M. A.; Patterson, H. H.; Tripp, C. P. *J. Phys. Chem. B* **2002**, *106*, 10058. (e) Rawashdeh-Omary, M. A.; Larochelle, C. L.; Patterson, H. H. *Inorg. Chem.* **2000**, *39*, 4527.
- (8) (a) Vickery, J. C.; Olmstead, M. M.; Fung, E. Y.; Balch, A. L. *Angew. Chem., Int. Ed. Engl.* **1997**, *36*, 1179. (b) Fung, E. Y.; Olmstead, M. M.; Vickery, J. C.; Balch, A. L. *Coord. Chem. Rev.* **1998**, *171*, 151. (c) Olmstead, M. M.; Jiang, F.; Attar, S.; Balch, A. L. *J. Am. Chem. Soc.* **2001**, *123*, 3260.
- (9) (a) Coker, N. L.; Krause Bauer, J. A.; Elder, R. C. *J. Am. Chem. Soc.* **2004**, *126*, 12. (b) Arvapally, R. K.; Sinha, P.; Hettiarachchi, S. R.; Coker, N. L.; Bedel, C. E.; Patterson, H. H.; Elder, R. C.; Wilson, A. K.; Omary, M. A. *J. Phys. Chem. C* **2007**, *111*, 10689.
- (10) Yam, V. W.-W.; Li, C. K.; Chan, C. L. *Angew. Chem., Int. Ed.* **1998**, *37*, 2857.

Chart 1. $[\text{Au}\{\text{C}(\text{NHMe})_2\}_2]^+$: *Syn* and *Anti* Rotomers

set of $\sigma(1)$ and $\sigma^*(2)$ MOs along with the collinear interaction of the p_z orbitals to form empty $\sigma_p(3)$ and $\sigma_p^*(4)$ MOs.^{11–13} Symmetry-allowed mixing of the filled $\sigma(1)$ and $\sigma^*(2)$ MOs and the empty $\sigma_p(3)$ and $\sigma_p^*(4)$ MOs stabilizes the filled $\sigma(1)$ and $\sigma^*(2)$ orbitals. Consequently, there is a net bonding interaction between the two metal centers.

Colorless, nonluminescent solutions of the two-coordinate complex $[\text{Au}\{\text{C}(\text{NHMe})_2\}_2]^+$, whose structure is shown in Chart 1, become intensely luminescent when frozen in a liquid N_2 bath.¹⁴ Strikingly, the colors of the emissions differ when various solvents are used. A frozen acetonitrile solution produces a green luminescence, whereas with frozen dimethyl sulfoxide or pyridine solutions the emission is blue. Frozen acetone solutions produce an orange luminescence, but with dimethylformamide no luminescence was observed. The emissions appear only after the solvent has frozen. The process is entirely reversible, warming the samples results in the loss of the luminescence while refreezing restores the colors. These colors are produced at different temperatures as each solvent freezes.

The cation $[\text{Au}\{\text{C}(\text{NHMe})_2\}_2]^+$ is readily prepared by reacting tetrachloroauric acid with methyl isocyanide and methyl amine in aqueous solution.¹⁵ Addition of a salt with the appropriate anion results in precipitation of colorless crystals of $[\text{Au}\{\text{C}(\text{NHMe})_2\}_2](\text{Anion})$.^{14,15}

Solid $[\text{Au}\{\text{C}(\text{NHMe})_2\}_2](\text{PF}_6) \cdot 0.5(\text{acetone})$ is also luminescent, and its luminescence has been attributed to the formation of extended chains of gold(I) centers that are connected through aurophilic attractions. Crystallographic studies of $[\text{Au}\{\text{C}(\text{NHMe})_2\}_2](\text{BF}_4)$, which is also luminescent, and $[\text{Au}\{\text{C}(\text{NHMe})_2\}_2](\text{PF}_6) \cdot 0.5(\text{acetone})$ reveal that both involve extended chains of cations and that the anions are hydrogen bonded to the cations through cation N–H groups. However, these chains differ in the $\text{Au} \cdots \text{Au}$

separations in each and in the carbene ligand orientations. In contrast, $[\text{Au}\{\text{C}(\text{NMe}_2)(\text{NHMe})\}_2](\text{PF}_6)$ forms a colorless, nonluminescent solid, in which there are no $\text{Au} \cdots \text{Au}$ interactions, a factor which supports the contention that aggregated species are responsible for the luminescence of $[\text{Au}\{\text{C}(\text{NHMe})_2\}_2](\text{PF}_6) \cdot 0.5(\text{acetone})$ in the solid state and in frozen solutions. The structural and luminescent properties of $[\text{Au}\{\text{C}(\text{NHMe})_2\}_2]\text{Cl} \cdot \text{H}_2\text{O}$ and $[\text{Au}\{\text{C}(\text{NHMe})_2\}_2]\text{Br} \cdot \text{H}_2\text{O}$, which contain isolated pairs of cations, have been reported.¹⁶

Here, we report studies directed toward understanding the factors responsible for the various colors of the emission resulting from crystals and frozen solutions that contain the cation $[\text{Au}\{\text{C}(\text{NHMe})_2\}_2]^+$. Although we have not been able to obtain a crystalline solid of this cation that displays the orange luminescence seen in frozen acetone solutions, we have been able to obtain crystals that display either a blue or a green emission. Blue luminescent materials are the weak link in the development of certain organic light-emitting diodes, and the development of new blue-emitting compounds is an important goal for that technology.¹⁷ We have utilized three similarly shaped anions of varying sizes ($(\text{PF}_6)^-$, $(\text{AsF}_6)^-$, and $(\text{SbF}_6)^-$) to explore how cation/anion interactions can influence the structure for a cation with multiple hydrogen bond donor sites and have discovered how solvate formation influences the structure.

Results

Colorless $[\text{Au}\{\text{C}(\text{NHMe})_2\}_2](\text{AsF}_6)$ is soluble in methanol, ethanol, acetonitrile, dimethylsulfoxide, and acetone. The salt has negligible solubility in dichloromethane, chloroform, chlorobenzene, diethyl ether, water, and hydrocarbons (pentane, hexane, benzene). Depending upon the conditions of crystallization, $[\text{Au}\{\text{C}(\text{NHMe})_2\}_2](\text{AsF}_6)$ forms colorless crystals with either a blue or a green luminescence as can be seen in Figure 1. This figure shows a photograph of two tubes containing $[\text{Au}\{\text{C}(\text{NHMe})_2\}_2](\text{AsF}_6)$ taken under irradiation with UV light. The tube on the right contains crystals grown by diffusion of pentane into an acetone solution of the salt, while the tube on the left contains crystals grown by diffusion of chlorobenzene into a 3-pentanone solution of the complex.

Structure of Blue-Glowing $[\text{Au}\{\text{C}(\text{NHMe})_2\}_2](\text{AsF}_6) \cdot 0.5(\text{benzene})$. This salt was obtained by placing an acetone solution of the complex over a layer of benzene. The salt crystallized as the two solutions diffused together. Crystal data for this and other new compounds are collected in Table 1. The structure of the cation in $[\text{Au}\{\text{C}(\text{NHMe})_2\}_2](\text{AsF}_6) \cdot 0.5(\text{benzene})$ is shown in Figure 2. The planar cation has crystallographic C_{2h} symmetry with the gold ion residing at a center of symmetry. Consequently, the cation has the *anti* rotameric orientation (see Chart 1) of the two carbene

(11) Roundhill, D. M.; Gray, H. B.; Che, C.-M. *Acc. Chem. Res.* **1989**, *22*, 55.

(12) Zipp, A. P. *Coord. Chem. Rev.* **1988**, *84*, 47.

(13) Mann, K. R.; Gordon, J. G., II; Gray, H. B. *J. Am. Chem. Soc.* **1975**, *97*, 3553.

(14) White-Morris, R. L.; Olmstead, M. M.; Jiang, F.; Tinti, D. S.; Balch, A. L. *J. Am. Chem. Soc.* **2002**, *124*, 2327.

(15) Parks, J. E.; Balch, A. L. *J. Organomet. Chem.* **1974**, *71*, 453.

(16) White-Morris, R. L.; Olmstead, M. M.; Jiang, F.; Balch, A. L. *Inorg. Chem.* **2002**, *41*, 2313.

(17) Wen, S.-W.; Lee, M.-T.; Chen, C. H. *J. Display Technol.* **2005**, *1*, 90.



Figure 1. Photograph of two tubes containing $[\text{Au}\{\text{C}(\text{NHMe})_2\}_2](\text{AsF}_6)$ taken under irradiation with UV light. The tube on the right contains crystals of $[\text{Au}\{\text{C}(\text{NHMe})_2\}_2](\text{AsF}_6)\cdot 0.5(\text{acetone})$ grown by diffusion of a layer of pentane on the top into an acetone solution of the salt at the bottom of the tube. The tube on the left contains crystals of $[\text{Au}\{\text{C}(\text{NHMe})_2\}_2](\text{EF}_6)\cdot 0.5(\text{chlorobenzene})$ grown by diffusion of chlorobenzene on the bottom of the tube into a 3-pentanone solution of the complex, which was placed over the chlorobenzene layer.

ligands. Selected bond distances within an individual cation are given in the caption to Figure 2.

The cations pack into extended, linear chains along a crystallographic 4_2 screw axis as seen in Figure 3. The $\text{Au}\cdots\text{Au}$ separation is 3.1871(2) Å. Thus, the carbene ligands on adjacent cations have staggered orientations. Importantly, the ligands of three adjacent cations are linked through hydrogen bonds with the fluorine atoms of one anion. These hydrogen bonds involve the inner N–H group of one ligand, which is bonded to a fluorine atom (F3) of an anion, and the outer N–H group of the cations above and below, which are bonded to fluorine atoms (F1 or F1a) of the same hexafluoroarsenate ion as seen in Figure 2. In addition to the orientation of the anions shown in Figure 2, there is a minor (0.1 site occupancy) orientation of the anion, which is not shown in Figure 2.

Figure 4 shows how the columns of cations with the associated anions are arranged around channels that contain the solvate molecule, benzene. The benzene molecules are disordered and occupy two superimposed sites with equal occupancy. There are no notable structural interactions of the solvate molecules with the cations or anions.

Structures of Blue-Glowing $[\text{Au}\{\text{C}(\text{NHMe})_2\}_2](\text{EF}_6)\cdot 0.5(\text{acetone})$, $E = \text{P}$ or As . As the crystal data in Table 1 show, these two salts are isostructural and crystallize in the

tetragonal space group $P4_2/mnm$. The structure of one member of this family, $[\text{Au}\{\text{C}(\text{NHMe})_2\}_2](\text{PF}_6)\cdot 0.5(\text{acetone})$, has been described previously and is similar to that of $[\text{Au}\{\text{C}(\text{NHMe})_2\}_2](\text{AsF}_6)\cdot 0.5(\text{benzene})$ discussed above. In $[\text{Au}\{\text{C}(\text{NHMe})_2\}_2](\text{EF}_6)\cdot 0.5(\text{acetone})$, the anions are fully ordered, whereas they are disordered in $[\text{Au}\{\text{C}(\text{NHMe})_2\}_2](\text{AsF}_6)\cdot 0.5(\text{benzene})$. Within the pair of $[\text{Au}\{\text{C}(\text{NHMe})_2\}_2](\text{EF}_6)\cdot 0.5(\text{acetone})$ compounds, the $\text{Au}\cdots\text{Au}$ separations vary as the sizes of the anions change. Thus, for $E = \text{P}$ the $\text{Au}\cdots\text{Au}$ separation is 3.1882(1) Å, while for $E = \text{As}$ it is longer, 3.2138(3) Å. These changes correspond to the changes in the E–F distances that parallel the screw axis, which are 1.607(5) Å for P–F and 1.7179(18) Å for As–F.

In the $[\text{Au}\{\text{C}(\text{NHMe})_2\}_2](\text{EF}_6)\cdot 0.5(\text{acetone})$, the acetone molecules, which are disordered with respect to a site of mmm symmetry, reside in a channel corresponding to the one occupied by the benzene molecules shown in Figure 4. The carbonyl groups of the acetone molecules, which lie in the center of the solvate cavity, are aligned parallel to the chains of gold ions. There are no hydrogen bonds between the acetone molecules and their surroundings.

We have also observed that tetrahydrofuran, dioxane, and cyclopentane also form solvated crystals that are isostructural with $[\text{Au}\{\text{C}(\text{NHMe})_2\}_2](\text{AsF}_6)\cdot 0.5(\text{benzene})$ and $[\text{Au}\{\text{C}(\text{NHMe})_2\}_2](\text{AsF}_6)\cdot 0.5(\text{acetone})$.¹⁸

Structure of Green-Glowing $[\text{Au}\{\text{C}(\text{NHMe})_2\}_2](\text{AsF}_6)\cdot 0.5(\text{chlorobenzene})$. Colorless crystals were obtained by placing a layer of chlorobenzene at the bottom of a 5 mm diameter glass tube and carefully adding a solution of the complex in 3-pentanone over the chlorobenzene layer. The data for crystals of the chlorobenzene solvate were refined in the tetragonal space group $P4_2/mmc$. Figure 5 shows a drawing of a portion of this solid. The solid consists of linear extended chains of cations with hydrogen bonding through the N–H groups to the fluorine atoms of the anions as found for the blue-glowing crystals of $[\text{Au}\{\text{C}(\text{NHMe})_2\}_2](\text{EF}_6)\cdot 0.5(\text{acetone})$. However, in the chlorobenzene solvate the cations are disordered as shown in Figure 5. There are two, equally populated orientations of the cation that are mirror images of each other and are separated by 36.9(6)°. Both lie in a common plane and have crystallographic C_{2h} symmetry. Each of these cations has the *anti* rotameric orientation. N2 is the only ligand atom that is common to both orientations.

The cations are again stacked into extended chains along a crystallographic 4_2 screw axis. However, the presence of disorder in the position of the ligand indicates that the staggered arrangement of the ligands generated by the 4_2 screw axis does not persist along the entire chain. The $\text{Au}\cdots\text{Au}$ separation in the chlorobenzene solvate is 3.203(2) Å, which is a value that is similar to the $\text{Au}\cdots\text{Au}$ distance, 3.1871(2) Å, in the corresponding benzene solvate.

As with $[\text{Au}\{\text{C}(\text{NHMe})_2\}_2](\text{AsF}_6)\cdot 0.5(\text{benzene})$ and with the $[\text{Au}\{\text{C}(\text{NHMe})_2\}_2](\text{EF}_6)\cdot 0.5(\text{acetone})$, $E = \text{P}$ or As , the cations and anions in the chlorobenzene solvate are situated around channels that contain chlorobenzene molecules.

(18) Pham, D. M. Ph.D. Thesis, University of California, Davis, 2007.

Table 1. Crystal Data and Data Collection Parameters for Salts of $[\text{Au}\{\text{C}(\text{NHMe})_2\}_2]^+$

	$[\text{Au}\{\text{C}(\text{NHMe})_2\}_2](\text{AsF}_6) \cdot 0.5(\text{benzene})$	$[\text{Au}\{\text{C}(\text{NHMe})_2\}_2](\text{PF}_6) \cdot 0.5(\text{acetone})^c$	$[\text{Au}\{\text{C}(\text{NHMe})_2\}_2](\text{AsF}_6) \cdot 0.5(\text{acetone})$	$[\text{Au}\{\text{C}(\text{NHMe})_2\}_2](\text{AsF}_6) \cdot 0.5(\text{chlorobenzene})$
formula	$\text{C}_9\text{H}_{19}\text{AsAuF}_6\text{N}_4$	$\text{C}_{7.5}\text{H}_{19}\text{AuF}_6\text{N}_4\text{O}_{0.5}\text{P}$	$\text{C}_{7.5}\text{H}_{19}\text{AsAuF}_6\text{N}_4\text{O}_{0.5}$	$\text{C}_9\text{H}_{18.5}\text{AsAuClF}_6\text{N}_4$
formula weight	569.17	515.20	559.15	585.88
<i>T</i> , K	90(2)	90(2)	90(2)	90(2)
color and habit	colorless needle	colorless needle	colorless needle	colorless needle
crystal system	tetragonal	tetragonal	tetragonal	tetragonal
space group	$P4_2/mnm$	$P4_2/mnm$	$P4_2/mnm$	$P4_2/mmc$
<i>a</i> , Å	15.9560(3)	15.4419(6)	15.6093(12)	11.1918(3)
<i>b</i> , Å	15.9560(3)	15.4419(6)	15.6093(12)	11.1918(3)
<i>c</i> , Å	6.3742(2)	6.3764(2)	6.4275(5)	6.4062(4)
α , deg	90	90	90	90
β , deg	90	90	90	90
γ , deg	90	90	90	90
<i>V</i> , Å ³	1622.83(7)	1520.47(10)	1566.1(2)	802.42(6)
radiation (λ , Å)	Mo K α (0.71073)	Mo K α (0.71073)	Mo K α (0.71073)	Mo K α (0.71073)
<i>Z</i>	4	4	4	2
d_{calcd} , g·cm ⁻³	2.317	2.251	2.367	2.425
μ , mm ⁻¹	11.146	9.842	11.550	11.356
unique data	1151	1402	1113	601
restraints	7	2	0	0
params. refined	85	86	73	50
R1 ^a	0.017	0.016	0.017	0.026
wR2 ^b	0.037	0.041	0.045	0.082

	$[\text{Au}\{\text{C}(\text{NHMe})_2\}_2](\text{PF}_6)$	$[\text{Au}\{\text{C}(\text{NHMe})_2\}_2](\text{AsF}_6)$	$[\text{Au}\{\text{C}(\text{NHMe})_2\}_2](\text{SbF}_6)$
formula	$\text{C}_6\text{H}_{16}\text{AuF}_6\text{N}_4\text{P}$	$\text{C}_6\text{H}_{16}\text{AsAuF}_6\text{N}_4$	$\text{C}_6\text{H}_{16}\text{AuF}_6\text{N}_4\text{Sb}$
formula weight	486.16	530.11	576.94
<i>T</i> , K	90(2)	90(2)	90(2)
color and habit	colorless prism	colorless prism	colorless needle
crystal system	orthorhombic	orthorhombic	monoclinic
space group	$Pnma$	$Pnma$	$P2_1/c$
<i>a</i> , Å	19.8652(15)	20.1461(17)	10.125(2)
<i>b</i> , Å	6.7447(5)	6.6955(6)	6.8885(15)
<i>c</i> , Å	10.1085(8)	10.2929(9)	20.667(5)
α , deg	90	90	90
β , deg	90	90	94.552(3)
γ , deg	90	90	90
<i>V</i> , Å ³	1354.39(18)	1388.4(2)	1436.9(5)
radiation (λ , Å)	Mo K α (0.71073)	Mo K α (0.71073)	Mo K α (0.71073)
<i>Z</i>	4	4	4
d_{calcd} , g·cm ⁻³	2.364	2.517	2.667
μ , mm ⁻¹	11.038	13.018	12.134
unique data	2196	1865	3275
restraints	0	0	0
params. refined	106	106	164
R1 ^a	0.032	0.017	0.049
wR2 ^b	0.075	0.042	0.134

^a For data with $I > 2\sigma I$. R1 = $(\sum ||F_o| - |F_c||) / \sum |F_o|$. ^b For all data. wR2 = $[(\sum w(F_o^2 - F_c^2)^2) / \sum w(F_o^2)^2]^{1/2}$. ^c Data from White-Morris, R. L.; Olmstead, M. M.; Jiang, F.; Tinti, D. S.; Balch, A. L. *J. Am. Chem. Soc.* **2002**, *124*, 2327.

Figure 6 shows a stereoview of the columns and the channel where the chlorobenzene molecules reside. These solvate molecules are disordered as shown at the bottom of Figure 6.

Attempts to transform the green-glowing crystals of $[\text{Au}\{\text{C}(\text{NHMe})_2\}_2](\text{AsF}_6) \cdot 0.5(\text{chlorobenzene})$ into blue-glowing crystals of $[\text{Au}\{\text{C}(\text{NHMe})_2\}_2](\text{AsF}_6) \cdot 0.5(\text{benzene})$ by immersing crystals of the former in benzene were unsuccessful. Similarly, blue-glowing crystals of $[\text{Au}\{\text{C}(\text{NHMe})_2\}_2](\text{AsF}_6) \cdot 0.5(\text{benzene})$ retained their blue luminescence when immersed in chlorobenzene.

Structures of Blue-Glowing, Solvate-Free $[\text{Au}\{\text{C}(\text{NHMe})_2\}_2](\text{EF}_6)$, E = P, As. Solvate-free crystals of $[\text{Au}\{\text{C}(\text{NHMe})_2\}_2](\text{PF}_6)$, and $[\text{Au}\{\text{C}(\text{NHMe})_2\}_2](\text{AsF}_6)$ have been obtained by crystallization of the salt from mixtures of methanol and water. As the data in Table 1 show, these two solvate-free salts are isostructural but the $(\text{SbF}_6)^-$ analogue is not (vide infra). Figure 7 shows a drawing of the cation,

which adopts the *syn* rotameric orientation, not the *anti* orientation seen in the solvates described above. Both of the outer N–H groups of the anion form hydrogen bonds to different fluorine atoms of one neighboring anion, while the inner N–H groups form hydrogen bonds to two other anions.

The cations self-associate again in columns as shown in Figure 8. In this case, however, one anion hydrogen bonds to only one cation in a particular chain; the linking of three cations in a chain to a common anion through N–H...F bonding (as seen in Figures 3 and 5 for the solvated crystals) is absent. The Au...Au separation is 3.3794(3) Å for the $(\text{PF}_6)^-$ salt, but it is slightly shorter, 3.3555(3) Å, for the $(\text{AsF}_6)^-$ salt. This trend is the reverse of what was seen for $[\text{Au}\{\text{C}(\text{NHMe})_2\}_2](\text{PF}_6) \cdot 0.5(\text{acetone})$ and $[\text{Au}\{\text{C}(\text{NHMe})_2\}_2](\text{AsF}_6) \cdot 0.5(\text{acetone})$ where the Au...Au distance was greater in the $(\text{AsF}_6)^-$ salt. In those solvated salts, the anions were hydrogen bonded to three cations and the F–P–F or

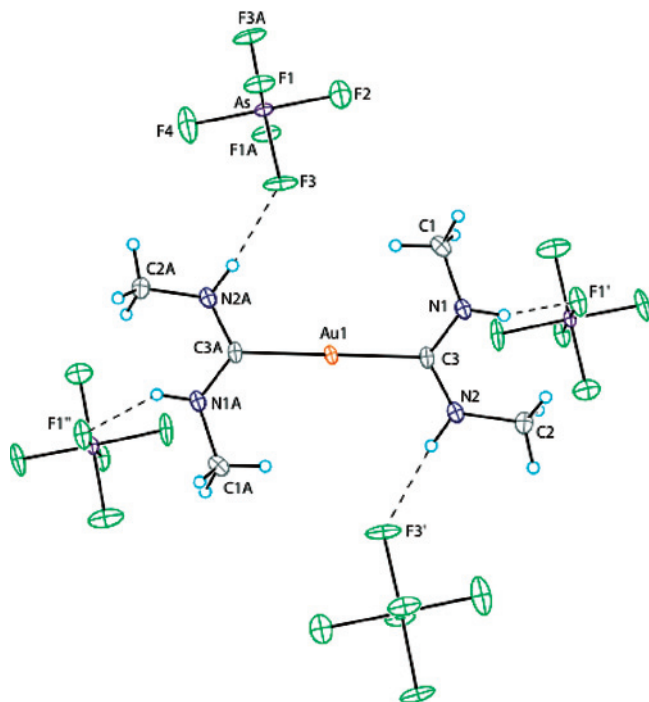


Figure 2. Drawing of the cation in $[\text{Au}\{\text{C}(\text{NHMe})_2\}_2](\text{AsF}_6) \cdot 0.5(\text{benzene})$ and its relationship to the neighboring anions. Relevant interatomic distances are: $\text{Au1}-\text{C3}$, 2.043(3); $\text{C3}-\text{N1}$, 1.316(5); $\text{C3}-\text{N2}$, 1.330(5); $\text{N1} \cdots \text{F1}'$, 3.046(3); $\text{N2} \cdots \text{F3}'$, 2.969(5) Å.

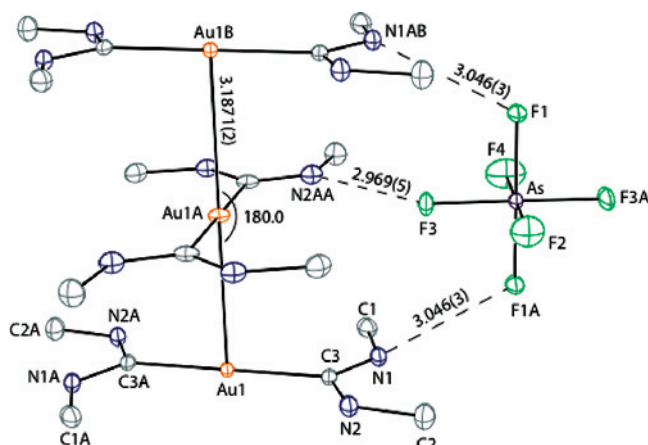


Figure 3. Drawing of the column of cations and the adjacent anions in crystalline $[\text{Au}\{\text{C}(\text{NHMe})_2\}_2](\text{AsF}_6) \cdot 0.5(\text{benzene})$.

F–As–F units were oriented parallel to the chain of cations. For the solvate-free salts, the anions interact with only one cation in a particular chain. Consequently, the size of the anion has no direct impact on the $\text{Au} \cdots \text{Au}$ separation along the chain of cations. These columns in the solvate-free $[\text{Au}\{\text{C}(\text{NHMe})_2\}_2](\text{PF}_6)$ and $[\text{Au}\{\text{C}(\text{NHMe})_2\}_2](\text{AsF}_6)$ are not linear, but are slightly kinked with an $\text{Au} \cdots \text{Au} \cdots \text{Au}$ angle of $172.579(15)^\circ$ in the $(\text{PF}_6)^-$ salt and $172.227(10)^\circ$ in the $(\text{AsF}_6)^-$ salt. Moreover, the cations in these solvate-free crystals have eclipsed ligand orientations.

The solvate-free crystals lack the channels found in solvated crystals as the drawing in Figure 9 reveals.

Structures of Solvate-Free $[\text{Au}\{\text{C}(\text{NHMe})_2\}_2](\text{SbF}_6)$. Colorless needles of solvate-free $[\text{Au}\{\text{C}(\text{NHMe})_2\}_2](\text{SbF}_6)$ were grown by slow diffusion of benzene into a concentrated

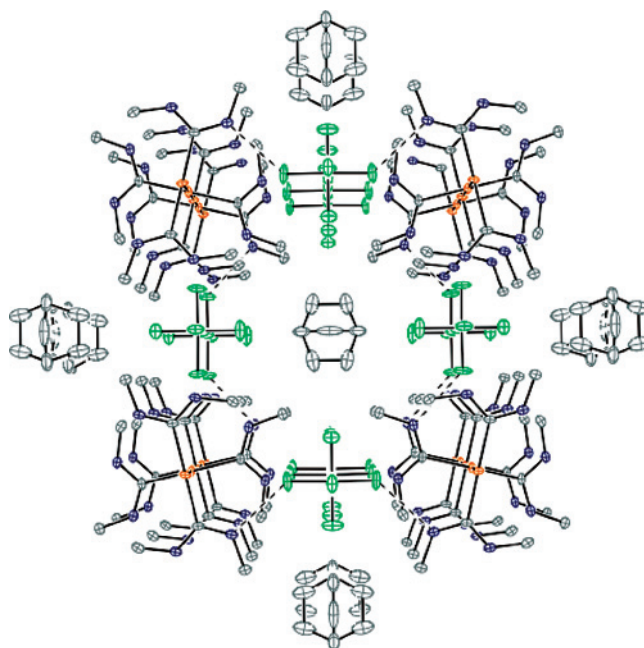


Figure 4. View of the structure of crystalline $[\text{Au}\{\text{C}(\text{NHMe})_2\}_2](\text{AsF}_6) \cdot 0.5(\text{benzene})$ that shows the location of the channel of disordered benzene molecules between the columns of gold-containing cations. There are two equally populated orientations for the benzene molecules and both are shown.

solution of the complex in 3-pentanone. Notice that this procedure, when applied to $[\text{Au}\{\text{C}(\text{NHMe})_2\}_2](\text{AsF}_6)$, produced the solvate $[\text{Au}\{\text{C}(\text{NHMe})_2\}_2](\text{AsF}_6) \cdot 0.5(\text{benzene})$. Curiously, solvate-free $[\text{Au}\{\text{C}(\text{NHMe})_2\}_2](\text{SbF}_6)$ forms a different structure from those of the solvate-free $(\text{PF}_6)^-$ and $(\text{AsF}_6)^-$ analogues. As with solvate-free $[\text{Au}\{\text{C}(\text{NHMe})_2\}_2](\text{PF}_6)$ and $[\text{Au}\{\text{C}(\text{NHMe})_2\}_2](\text{AsF}_6)$, the cation adopts the *syn* rotameric orientation and there is a similar but not identical hydrogen bonding pattern (see Figure S11).

As with all the structures considered here, the cations are arranged in columns as shown in Figure 10. In these columns, there are two $\text{Au} \cdots \text{Au}$ separations of 3.4888(9) and 3.5379(9) Å. The columns are strongly kinked with a $\text{Au} \cdots \text{Au} \cdots \text{Au}$ angle of $157.231(19)^\circ$.

Figure 11 shows the overall organization of the solid, which does not contain any channels of the type seen in the solvated crystals. Comparison of Figures 8 (which is relevant for the $(\text{PF}_6)^-$ and $(\text{AsF}_6)^-$ salts) and 11 (for the $(\text{SbF}_6)^-$ salt) reveals how different the packing is within the two different types of solvate-free salts.

Luminescence from Crystalline Samples. Data regarding the luminescence of the salts are set out in Table 2. Emission and excitation spectra for crystals of blue-glowing $[\text{Au}\{\text{C}(\text{NHMe})_2\}_2](\text{AsF}_6) \cdot 0.5(\text{benzene})$, green-glowing $[\text{Au}\{\text{C}(\text{NHMe})_2\}_2](\text{AsF}_6) \cdot 0.5(\text{chlorobenzene})$, and blue-glowing, solvate-free $[\text{Au}\{\text{C}(\text{NHMe})_2\}_2](\text{AsF}_6)$ obtained at 298 K are shown in Figure 12. The difference in the emission between blue-glowing $[\text{Au}\{\text{C}(\text{NHMe})_2\}_2](\text{AsF}_6) \cdot 0.5(\text{benzene})$ and green-glowing $[\text{Au}\{\text{C}(\text{NHMe})_2\}_2](\text{AsF}_6) \cdot 0.5(\text{chlorobenzene})$ is quite small, namely, a shift of only 10 nm toward the red for green-glowing $[\text{Au}\{\text{C}(\text{NHMe})_2\}_2](\text{AsF}_6) \cdot 0.5(\text{chlorobenzene})$. Clearly the human eye is sensitive to small spectral differences in this region. Solutions of salts

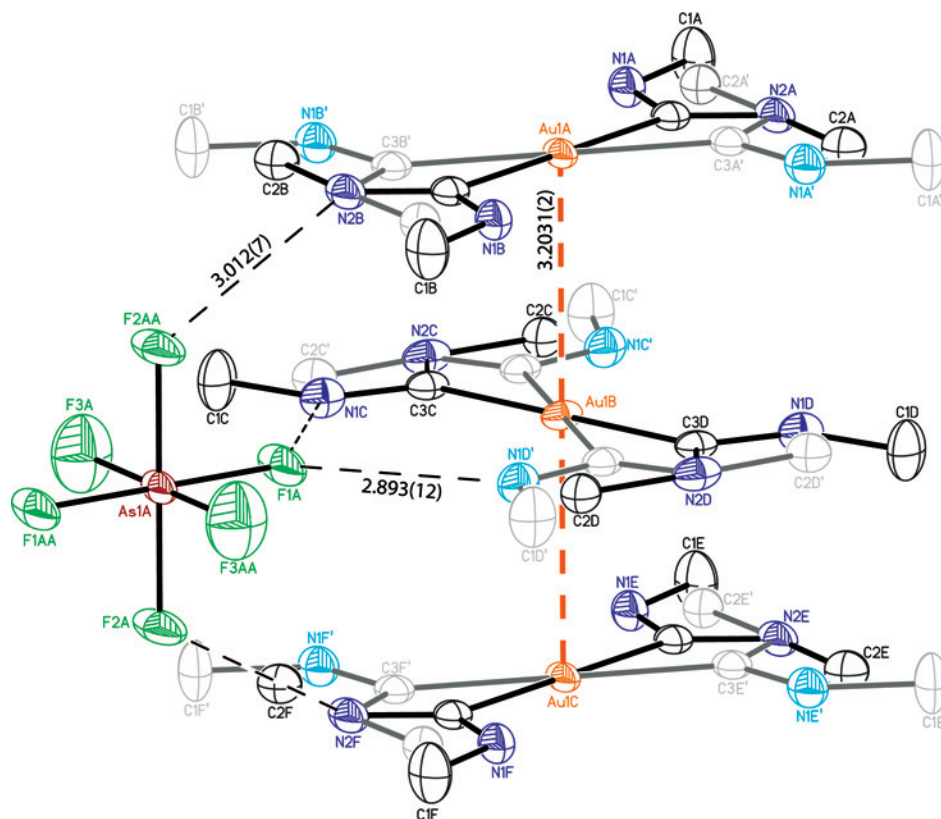


Figure 5. Drawing of the column of cations and the adjacent anions in crystalline $[\text{Au}\{\text{C}(\text{NHMe})_2\}_2](\text{AsF}_6)\cdot 0.5(\text{chlorobenzene})$. The cations are disordered over two, equally populated orientations. One orientation is denoted by using black lines to connect the atoms, while the other is shown with grey lines connecting the atoms.

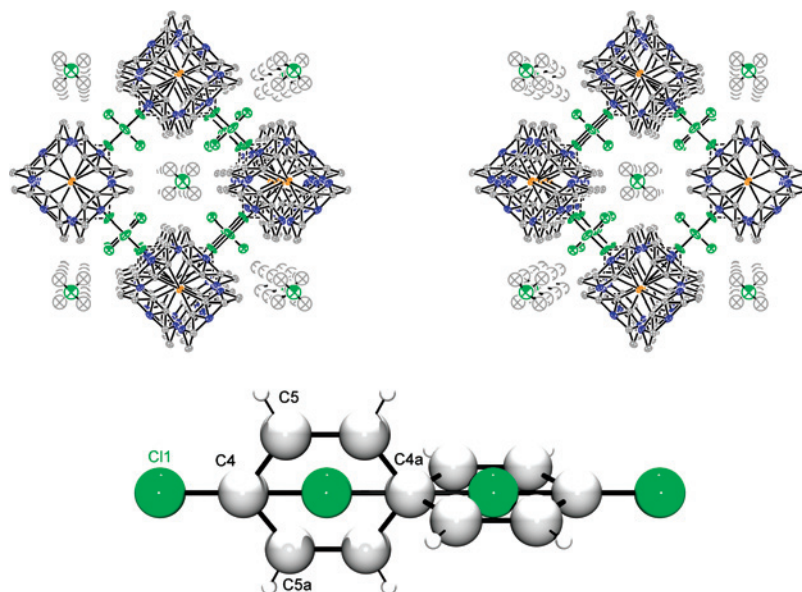


Figure 6. Top: a stereoview of the structure of crystalline $[\text{Au}\{\text{C}(\text{NHMe})_2\}_2](\text{AsF}_6)\cdot 0.5(\text{chlorobenzene})$ that shows the location of the channel of disordered chlorobenzene molecules between the columns of gold-containing cations and the adjacent anions. Bottom: the arrangement of the disordered chlorobenzene molecules in the channels within crystalline $[\text{Au}\{\text{C}(\text{NHMe})_2\}_2](\text{AsF}_6)\cdot 0.5(\text{chlorobenzene})$.

of $[\text{Au}\{\text{C}(\text{NHMe})_2\}_2]^+$ are non emissive and show an absorption maximum at 210 nm. However, all the spectra shown in Figure 12 have excitation maxima that occur at much lower energies. Thus, the emissive properties of the solids are due to the self-association of the cations and the resulting overlap of the gold d_z and p_z orbitals that lie parallel

to the chain axis. The excitation results from transfer of an electron from the filled band of gold d_z MOs into the empty band of gold p_z MOs, while emission reverses this process.

Figure 13 presents corresponding data for samples of $[\text{Au}\{\text{C}(\text{NHMe})_2\}_2](\text{AsF}_6)\cdot 0.5(\text{benzene})$, $[\text{Au}\{\text{C}(\text{NHMe})_2\}_2](\text{AsF}_6)\cdot 0.5(\text{chlorobenzene})$, and solvate-free $[\text{Au}\{\text{C}(\text{NHMe})_2\}_2](\text{AsF}_6)$ at

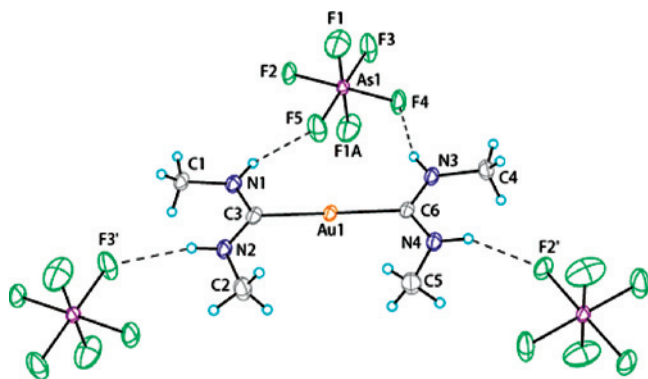


Figure 7. Drawing of the cation in solvate-free $[\text{Au}\{\text{C}(\text{NHMe})_2\}_2](\text{AsF}_6)$ and its relationship to the nearby anions. Relevant interatomic distances are: Au1–C3, 2.041(4); Au1–C6, 2.037(4); C3–N1, 1.333(6); C3–N2, 1.323(6); C6–N3, 1.333(6); C6–N4, 1.316(5); N1···F5, 2.955(5); N2···F3', 3.095(5); N3···F4, 2.981(5); and N4···F2', 2.919(5) Å.

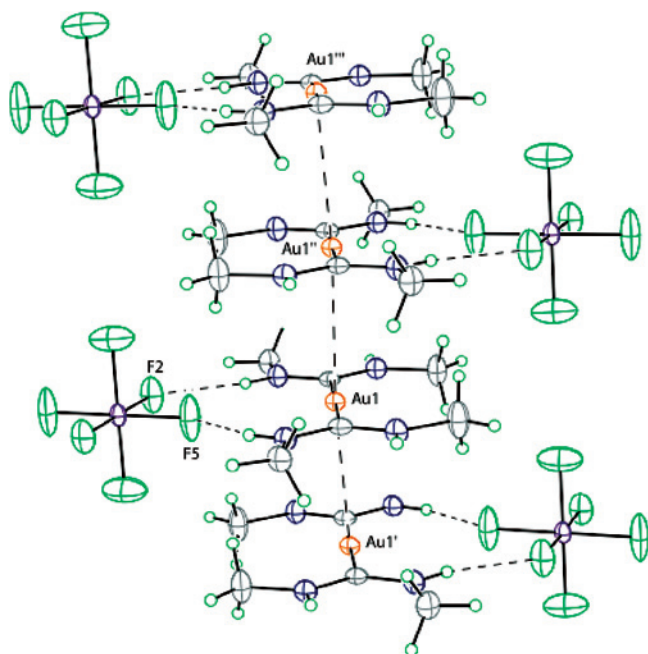


Figure 8. Drawing of the column of cations and the adjacent anions in solvate-free $[\text{Au}\{\text{C}(\text{NHMe})_2\}_2](\text{AsF}_6)$.

77 K. For $[\text{Au}\{\text{C}(\text{NHMe})_2\}_2](\text{AsF}_6) \cdot 0.5(\text{chlorobenzene})$ and solvate-free $[\text{Au}\{\text{C}(\text{NHMe})_2\}_2](\text{AsF}_6)$ cooling to 77 K produces two emission bands: one at about 528 nm and the other at about 455 nm. These are assigned to phosphorescence and fluorescence, respectively, on the basis of the differences in Stokes' shifts and prior work on $[\text{Au}\{\text{C}(\text{NHMe})_2\}_2](\text{PF}_6) \cdot 0.5(\text{acetone})$, which revealed that its low energy band has a μs lifetime whereas the high energy emission had a shorter (<100 ns) lifetime. For $[\text{Au}\{\text{C}(\text{NHMe})_2\}_2](\text{AsF}_6) \cdot 0.5(\text{benzene})$ only a single emission at 529 nm is observed at 77 K, and this is also assigned to phosphorescence.

Emission and excitation spectra for crystals of solvate free $[\text{Au}\{\text{C}(\text{NHMe})_2\}_2](\text{PF}_6)$, $[\text{Au}\{\text{C}(\text{NHMe})_2\}_2](\text{AsF}_6)$, and $[\text{Au}\{\text{C}(\text{NHMe})_2\}_2](\text{SbF}_6)$ are shown in the Supporting Information, and data are given in Table 2. The spectra of $[\text{Au}\{\text{C}(\text{NHMe})_2\}_2](\text{PF}_6)$ and $[\text{Au}\{\text{C}(\text{NHMe})_2\}_2](\text{AsF}_6)$ are quite similar, which is to be expected since both salts have very similar structures. The spectra from $[\text{Au}\{\text{C}(\text{NHMe})_2\}_2]-$

(SbF_6) differ with the emission occurring at lower energy. The greater bending of the columns of cations provides less overlap of the gold d_{z^2} and p_z orbitals along the chain. As a result, the energy gap between the filled d_{z^2} band and the empty p_z band is lower in the $(\text{SbF}_6)^-$ salt than in the $(\text{PF}_6)^-$ and $(\text{AsF}_6)^-$ salts, and the corresponding emission and excitation occur at higher energies.

^1H NMR Spectra of the Salts. To confirm the presence of solvate molecules in these salts, the ^1H NMR spectra of these compounds have been obtained in dimethyl sulfoxide- d_6 . All of the salts dissolve to give spectra that are indicative of the presence of the cation $[\text{Au}\{\text{C}(\text{NHMe})_2\}_2]^+$, which has resonances at 2.58 ppm (d, 3H with $J = 8$ Hz) and 3.096 ppm (d, 3H with $J = 8$ Hz) that are due to the two inequivalent methyl groups and resonances at 8.322 (q, 1H with $J = 8$ Hz) and 8.013 (q, 1H with $J = 8$ Hz) attributable to the inner and outer N–H protons. These data are similar to observations reported earlier for this cation. Identical sets of weaker methyl doublets at 2.60 ppm with $J = 9$ Hz and 3.05 ppm with $J = 7$ Hz along with broad N–H resonances at 8.073 and 8.417 ppm are also observed for all samples and appear to be due to the presence of minor amounts of ligands with both of the methyl groups in the inner or outer positions as shown in Chart 2. For $[\text{Au}\{\text{C}(\text{NHMe})_2\}_2](\text{AsF}_6) \cdot 0.5(\text{benzene})$, an additional singlet is seen at 7.33 ppm as a result of the benzene protons, whereas for $[\text{Au}\{\text{C}(\text{NHMe})_2\}_2](\text{AsF}_6) \cdot 0.5(\text{acetone})$ a singlet due to the acetone protons is seen at 2.06 ppm. With $[\text{Au}\{\text{C}(\text{NHMe})_2\}_2](\text{AsF}_6) \cdot 0.5(\text{chlorobenzene})$ a multiplet at 7.46–7.30 ppm is observed for the chlorobenzene molecules. These solvate resonances are absent in the ^1H NMR spectra obtained from unsolvated $[\text{Au}\{\text{C}(\text{NHMe})_2\}_2](\text{PF}_6)$, $[\text{Au}\{\text{C}(\text{NHMe})_2\}_2](\text{AsF}_6)$, and $[\text{Au}\{\text{C}(\text{NHMe})_2\}_2](\text{SbF}_6)$.

Discussion

The results presented here give further evidence that demonstrates how the self-association of the cation $[\text{Au}\{\text{C}(\text{NHMe})_2\}_2]^+$ and the luminescence of the resulting solids are altered when different anions are present and when solvate molecules are incorporated into the solid state.

Hydrogen bonding between the cations and anions is extensive in these structures. Although the anions $(\text{PF}_6)^-$ and $(\text{AsF}_6)^-$ can span three cations and facilitate the auriphilic interactions as seen in Figures 3 and 5, this arrangement does not extend to the solvate-free salts, where each anion interacts with only one cation of a particular column. Moreover, all our attempts to form crystals with $(\text{SbF}_6)^-$ spanning three cations have been unsuccessful. Thus, while we can expect that hydrogen bonding with the cations may help promote the formation of columnar structures, we cannot be assured that the arrangement shown in Figures 3 and 5 will pertain under other circumstances. In addition to linkages along columns, extensive linkages between the columns are made through hydrogen bonding between cations and anions as shown in Figures 4, 6, 9, and 11.

The presence of solvate molecules in some of the salts reported here produces channels to accommodate them. No hydrogen bonding occurs between these solvate molecules

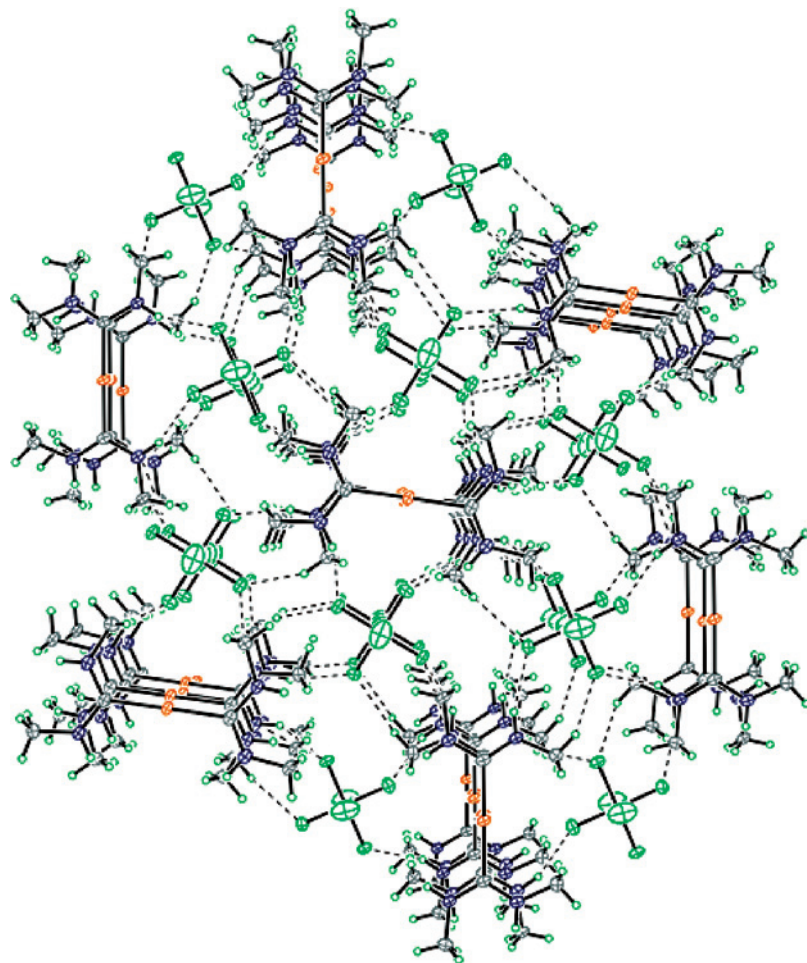


Figure 9. Drawing showing the packing between the columns of cations and the absence of a solvate channel in solvate-free $[\text{Au}\{\text{C}(\text{NHMe})_2\}_2](\text{AsF}_6)$.

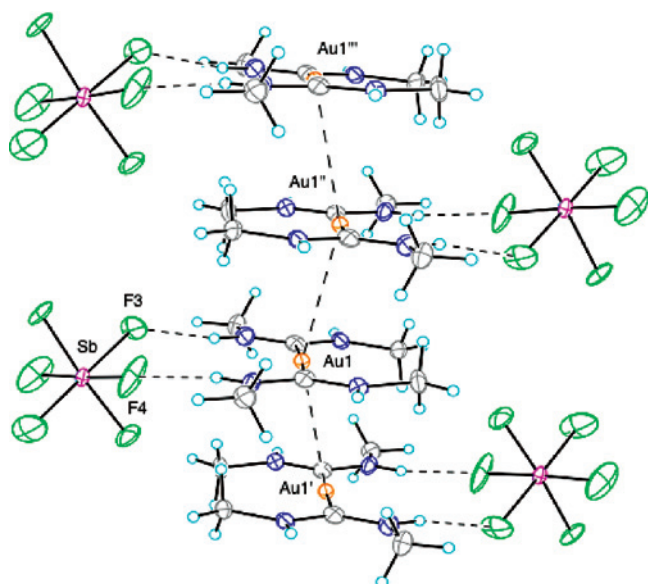


Figure 10. Drawing of the column of cations and the adjacent anions in solvate-free $[\text{Au}\{\text{C}(\text{NHMe})_2\}_2](\text{SbF}_6)$.

and their surroundings. Rather, they appear to simply occupy space between the columns of cations and anions. It is somewhat surprising that nonpolar molecules like benzene and cyclopentane can be trapped in such a salt. The solvate molecules also exert a subtle effect on the columnar

arrangement of the cations. While incorporation of benzene, acetone, cyclopentane, dioxane, and tetrahydrofuran produce blue-glowing crystals with ordered stacks of cations as shown in Figure 3, incorporation of chlorobenzene produces green-glowing crystals in which there is disorder in the cation positioning within the columns. It is this disorder in the columns that may be responsible for the slight shift in emission that results in the green emission from $[\text{Au}\{\text{C}(\text{NHMe})_2\}_2](\text{AsF}_6) \cdot 0.5(\text{chlorobenzene})$.

Experimental Section

Materials. Literature procedures were used for preparation of methyl isocyanide,^{19,20} $[\text{Au}\{\text{C}(\text{NHMe})_2\}_2](\text{PF}_6)$, $[\text{Au}\{\text{C}(\text{NHMe})_2\}_2](\text{AsF}_6)$, and $[\text{Au}\{\text{C}(\text{NHMe})_2\}_2](\text{SbF}_6)$.¹⁵

Crystal Growth. $[\text{Au}\{\text{C}(\text{NHMe})_2\}_2](\text{AsF}_6) \cdot 0.5(\text{benzene})$. Colorless needles were grown by slow diffusion of benzene into a solution of $[\text{Au}\{\text{C}(\text{NHMe})_2\}_2](\text{AsF}_6)$ in 3-pentanone. Upon heating, crystals of this compound started to turn gray at 165 °C and eventually melted at a melting range of 178–180 °C to give a brown melt that is not luminescent. IR: 537 m, 592 m, 675 sh, 695 sh, 1038 m, 1138 w, 1198 w, 1373 w, 1463 w, 2523 m, 1592 sh, 2953 w, 3394 vs (N–H), 3447 vs (N–H), cm^{-1} .

$[\text{Au}\{\text{C}(\text{NHMe})_2\}_2](\text{AsF}_6) \cdot 0.5(\text{acetone})$. Colorless needles were grown by slow diffusion of pentane to a concentrated solution of $[\text{Au}\{\text{C}(\text{NHMe})_2\}_2](\text{AsF}_6)$ in acetone. Crystals of this compound started to turn gray at 161 °C and eventually melted at a melting range of 170–172 °C to give a brown melt that is no

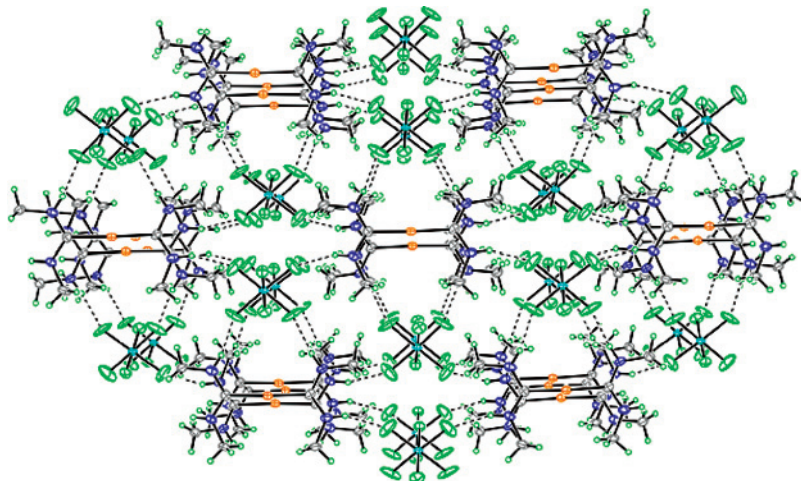


Figure 11. Drawing showing the packing of the columns of cations and neighboring anions and the absence of a solvate channel in solvate-free $[\text{Au}\{\text{C}(\text{NHMe})_2\}_2](\text{SbF}_6)$.

Table 2. Emission and Excitation data for Salts of $[\text{Au}\{\text{C}(\text{NHMe})_2\}_2]^+$

compound	emission (298 K), λ_{max} (nm)	excitation (298 K), λ_{max} (nm)	emission (77 K), λ_{max} (nm)	excitation (77 K), λ_{max} (nm)
$[\text{Au}\{\text{C}(\text{NHMe})_2\}_2](\text{AsF}_6) \cdot 0.5(\text{benzene})$	480	410	529	443
$[\text{Au}\{\text{C}(\text{NHMe})_2\}_2](\text{PF}_6) \cdot 0.5(\text{acetone})^a$	482	383	460, 530	365
$[\text{Au}\{\text{C}(\text{NHMe})_2\}_2](\text{AsF}_6) \cdot 0.5(\text{acetone})$	468	394	514	439
$[\text{Au}\{\text{C}(\text{NHMe})_2\}_2](\text{AsF}_6) \cdot 0.5(\text{chlorobenzene})$	490	405	528, 470	440
$[\text{Au}\{\text{C}(\text{NHMe})_2\}_2](\text{PF}_6)$	480	380	462, 535	415
$[\text{Au}\{\text{C}(\text{NHMe})_2\}_2](\text{AsF}_6)$	476	365	455, 526	416
$[\text{Au}\{\text{C}(\text{NHMe})_2\}_2](\text{SbF}_6)$	450	360	425, 460	360

^a Data from White-Morris, R. L.; Olmstead, M. M.; Jiang, F.; Tinti, D. S.; Balch, A. L. *J. Am. Chem. Soc.* **2002**, *124*, 2327.

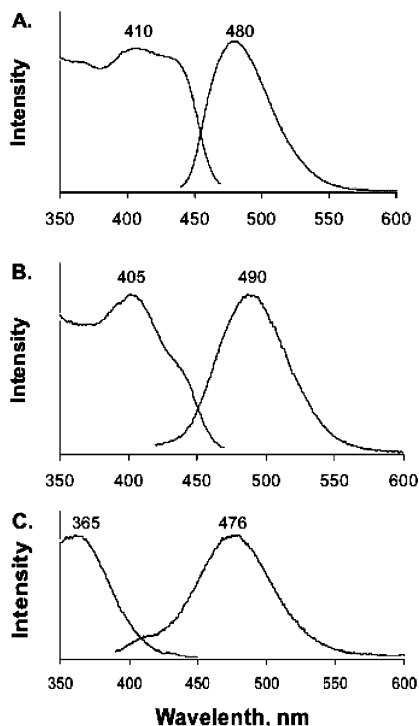


Figure 12. Emission (right) and excitation spectra (left) for crystalline samples of blue-glowing $[\text{Au}\{\text{C}(\text{NHMe})_2\}_2](\text{AsF}_6) \cdot 0.5(\text{benzene})$, green-glowing $[\text{Au}\{\text{C}(\text{NHMe})_2\}_2](\text{AsF}_6) \cdot 0.5(\text{chlorobenzene})$, and blue-glowing, solvate-free $[\text{Au}\{\text{C}(\text{NHMe})_2\}_2](\text{AsF}_6)$ at 298 K.

longer luminescent. IR: 691 sh, 1033 w, 1195 w, 1218 w, 1314 w, 1370 w, 1448 w, 1524 m, 1589 sh, 1685 w, 2950 w, 3388 vs (N–H), 3446 vs (N–H), cm^{-1} .

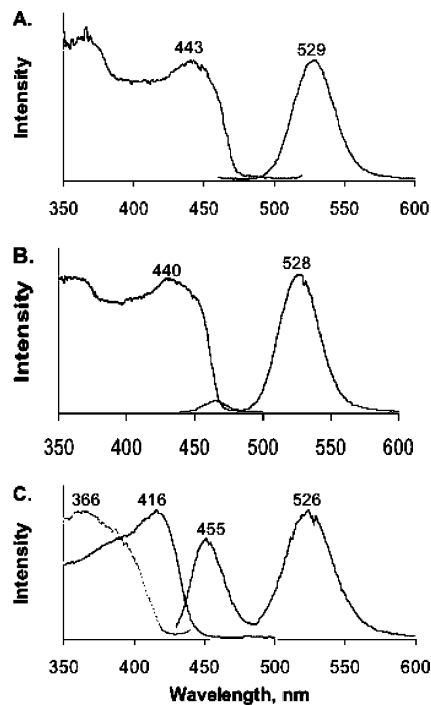
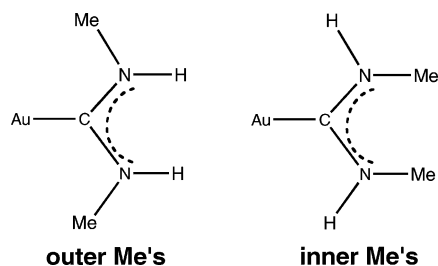


Figure 13. Emission (right) and excitation spectra (left) for crystalline samples of $[\text{Au}\{\text{C}(\text{NHMe})_2\}_2](\text{AsF}_6) \cdot 0.5(\text{benzene})$, $[\text{Au}\{\text{C}(\text{NHMe})_2\}_2](\text{AsF}_6) \cdot 0.5(\text{chlorobenzene})$, and solvate-free $[\text{Au}\{\text{C}(\text{NHMe})_2\}_2](\text{AsF}_6)$ at 77 K.

$[\text{Au}\{\text{C}(\text{NHMe})_2\}_2](\text{AsF}_6) \cdot 0.5(\text{chlorobenzene})$. Colorless crystals suitable for X-ray diffraction were grown by slow diffusion of chlorobenzene into a concentrated solution of $[\text{Au}\{\text{C}(\text{NHMe})_2\}_2](\text{AsF}_6)$.

Chart 2. $[\text{Au}\{\text{C}(\text{NHMe})_2\}_2]^+$: Alternate Ligand Conformations

(AsF₆) in 3-pentanone. IR: 675 sh, 694 sh, 1034 m, 1137 w, 1197 w, 1317 w, 1370 w, 1422 w, 1446 w, 1461 w, 1524 m, 1589 m, 2982, 3398 vs (N–H), 3446 vs (N–H), cm⁻¹.

Solvate-Free $[\text{Au}\{\text{C}(\text{NHMe})_2\}_2](\text{PF}_6)$, and $[\text{Au}\{\text{C}(\text{NHMe})_2\}_2](\text{AsF}_6)$. A 0.05 g sample of $[\text{Au}\{\text{C}(\text{NHMe})_2\}_2](\text{PF}_6)$ or $[\text{Au}\{\text{C}(\text{NHMe})_2\}_2](\text{AsF}_6)$ was dissolved in 5 mL of methanol and mixed with 5 mL of water. The resulting colorless solutions were filtered, transferred to 20 mL beakers, and allowed to evaporate slowly. X-ray quality crystals were grown after 24 h of slow evaporation. $[\text{Au}\{\text{C}(\text{NHMe})_2\}_2](\text{PF}_6)$ starts to become gray at 175 °C and eventually melts at 182–185° to give a brown melt. $[\text{Au}\{\text{C}(\text{NHMe})_2\}_2](\text{AsF}_6)$ starts to become gray at 170° and eventually melts at 179–181 °C to give a brown melt. IR spectrum for $[\text{Au}\{\text{C}(\text{NHMe})_2\}_2](\text{AsF}_6)$: 691 sh, 1033 w, 1195 w, 1218 w, 1314 w, 1370 w, 1448 w, 1524 m, 1589 m, 2980 w, 3388 vs ($\nu\text{N-H}$), 3446 vs ($\nu\text{N-H}$), cm⁻¹. IR spectrum for $[\text{Au}\{\text{C}(\text{NHMe})_2\}_2](\text{PF}_6)$: 686 w, 813 sh, 1054 w, 1175 w, 1231 w, 1325 w, 1395 w, 1451 w, 1524 w, 1588 m, 2978 w, 3391 vs ($\nu\text{N-H}$), 3448 vs ($\nu\text{N-H}$), cm⁻¹.

Solvate-Free $[\text{Au}\{\text{C}(\text{NHMe})_2\}_2](\text{SbF}_6)$. A 0.10 g (0.312 mmol) portion of (tht)AuCl was transferred to a 50 mL round-bottom flask and dissolved in 10 mL of acetonitrile. While stirring this colorless solution, 0.10 mL of methyl isocyanide was added and a white precipitate formed. After stirring the mixture for 20 min, 2.0 mL of 30% aqueous methyl amine was added and the white precipitate redissolved. Then 0.10 g (0.53 mmol) of NaSbF₆ in 10 mL of acetonitrile was added to form a cloudy solution. After stirring the mixture for 10 min, it was filtered. The filtrate was taken to dryness using a rotatory evaporator. The product was a colorless solid that displayed a blue luminescence under UV light: yield, 0.13 g (72%). Colorless needles suitable for X-ray diffraction were grown by slow diffusion of benzene into a concentrated solution of this salt in

3-pentanone. IR spectrum: 680 sh, 910 w, 1015 w, 1020 w, 1180 w, 1190 w, 1310 w, 1400 w, 1452 w, 1520 m, 1581 m, 2920 w, 3382 vs ($\nu\text{N-H}$), 3435 vs ($\nu\text{N-H}$), cm⁻¹.

X-ray Crystallography and Data Collection. The crystals were removed from the glass tubes in which they were grown together with a small amount of mother liquor and immediately coated with a hydrocarbon oil on the microscope slide. Suitable crystals were mounted on glass fibers with silicone grease and placed in the cold stream of a Bruker SMART CCD with graphite monochromated Mo K α radiation at 90(2) K. Check reflections were stable throughout the data collection. Crystal data are given in Table 2.

The structures were solved by Patterson methods and refined using all data (based on F^2) using the software of SHELXTL 5.1. A semiempirical method utilizing equivalents was employed to correct for absorption.²¹ Hydrogen atoms were added geometrically and refined with a riding model.

Physical Measurements. IR spectra were recorded as neat powders on a Mattson Genesis II FT-IR spectrometer fitted with a Specac ATR accessory. Electronic absorption spectra were recorded using a PharmaSpec UV-1700 UV–visible spectrophotometer. Spectra of solids were obtained from samples dispersed in Nujol mulls. Emission and excitation spectra were taken with a SPEX FluoroMax-3 Spectrofluorometer manufactured by Jobin Yvon/HORIBA.

Acknowledgment. We thank the Petroleum Research Fund (Grant) for support.

Supporting Information Available: Figures showing the cation in solvate-free $[\text{Au}\{\text{C}(\text{NHMe})_2\}_2](\text{SbF}_6)$ and the nearby anions, emission and excitation spectra for $[\text{Au}\{\text{C}(\text{NHMe})_2\}_2](\text{EF}_6)$ (E = P, As, Sb) at 298 K and at 77 K (PDF). X-ray crystallographic files in CIF format for $[\text{Au}\{\text{C}(\text{NHMe})_2\}_2](\text{AsF}_6) \cdot 0.5(\text{benzene})$, $[\text{Au}\{\text{C}(\text{NHMe})_2\}_2](\text{AsF}_6) \cdot 0.5(\text{acetone})$, $[\text{Au}\{\text{C}(\text{NHMe})_2\}_2](\text{AsF}_6) \cdot 0.5(\text{chlorobenzene})$, $[\text{Au}\{\text{C}(\text{NHMe})_2\}_2](\text{PF}_6)$, $[\text{Au}\{\text{C}(\text{NHMe})_2\}_2](\text{AsF}_6)$, and $[\text{Au}\{\text{C}(\text{NHMe})_2\}_2](\text{SbF}_6)$. This material is available free of charge via the Internet at <http://pubs.acs.org>.

IC702481V

- (19) Weber, W. P.; Gokel, G. W.; Ugi, I. K. *Angew. Chem., Int. Ed. Engl.* **1972**, *11*, 530.
 (20) Gokel, G. W.; Widera, R. P.; Weber, W. P. *Org. Synth.* **1976**, *55*, 96.
 (21) Sheldrick, G. M. *SADABS*, version 2.10; University of Göttingen: Germany, 2003.